≪Research Paper≫ Applied Science and Convergence Technology Vol.24 No.4, July 2015, pp.96~101
http://dx.doi.org/10.5757/ASCT.2015.24.4.96

Quantitative Evaluation on Photocatalytic Activity of Anatase TiO_2 Nanocrystals in Aqueous Solution

Byungwook Jeon and Yu Kwon Kim*

Department of Chemistry and Department of Energy Systems Research, Ajou University, Suwon 443-749, Korea

(Received July 20, 2015, Accepted July 29, 2015)

Quantitative evaluation of photocatalytic activity of oxide nanoparticles in aqueous solution is quite challenging in that the kinetic reaction rate is determined by a complicated interplay among various limiting factors such as light scattering and absorption, diffusion and adsorption of reactants in condensed liquid phase, photoexcited charge separation and recombination rate, and the exact nature of active sites determined by detailed morphology and crystallinity of nanocrystals. Here, we present our simple experimental results showing that the kinetic regime of a typical photocatalytic degradation experiment over UV-irradiated TiO_2 nanoparticles in aqueous solution is in that dominated by the photoactivity of TiO_2 and its concentration. This result lays a firm ground of using the measured kinetic reaction rate in evaluating photocatalytic efficiency of oxide nanocrystals under evaluation.

Keywords : Photocatalysis, TiO_2 nanocrystals, Reaction rate, Photodegradation, Methylene blue

I. Introduction

TiO_2 is a chemically stable oxide material under ambient condition with a bandgap of about 3 eV which can absorb UV light and induce fascinating photocatalytic processes [1–4] such as photooxidation of organic dyes [5–9] and water splitting [10–14] via photoexcited charge carriers [12,15,16]. This has initiated numerous researches on size and shape-controlled TiO_2 nanocrystals [17–27] and nanostructures [28–34]. However, the exact evaluation of photocatalytic activity of the oxide particles is often hampered by the complex interplay among various physicochemical processes imposed by the heterogeneous reaction condition at the liquid–solid interface coupled with photoexcitation and relaxation dynamics [13,35]. Under this condition, the factors that have an impact on the measured reaction rate could come from various unknown sources and the quantitative evaluation of the kinetic reaction rate is rarely performed since the rate is not simply related to the concentration of reactant under the reaction condition and the active sites are not well defined [13].

Here, we show our results on the quantitative evaluation of photocatalytic activity of shape-controlled TiO_2 nanocrystals. By measuring initial rate constant under a well-controlled reaction condition, we find that the photocatalytic reaction rate can be used to evaluate the properties of surfaces of the nanocrystals in connection with the active sites and

* [E-mail] yukwonkim@ajou.ac.kr

the efficiency of reaction rates induced by photogenerated hot carriers.

II. Experimental Details

1. Synthesis of TiO_2 nanocrystals

TiO_2 nanocrystals were synthesized by a hydrothermal method starting from tetrabutyltitanate (TBT, 25 g) in butanol (25 ml) and a concentrated HF aqueous solution (48 wt%, 4 ml) as described earlier [19]. After the reaction in an autoclave at 200°C for 24 h, white powders were collected by filtration, rinsing with deinonized water, and drying at 80°C. Post-annealing treatments were performed in a quartz tubing under O_2 atmosphere (1 atm, 50 sccm), which was kept at elevated temperatures (300～600°C) for 2 hours.

2. Characterization of TiO_2 nanocrystals

The SEM images of the as-synthesized TiO_2 powders shown in Fig. 1 clearly indicate a planar square shape with quite uniform size distribution. It confirms that TiO_2 nanocrystals with large {001} facets are reproducibly synthesized by the present synthetic method [36-38]. XRD (Rigaku, Ultima III) spectra were obtained using Cu Kα radiation (λ=0.15406 nm). EPR (JES-TE200, JEOL) spectra were taken by sweeping magnetic field under an X-band (9.43 GHz, 1.5 mW) microwave and at room temperature (RT).

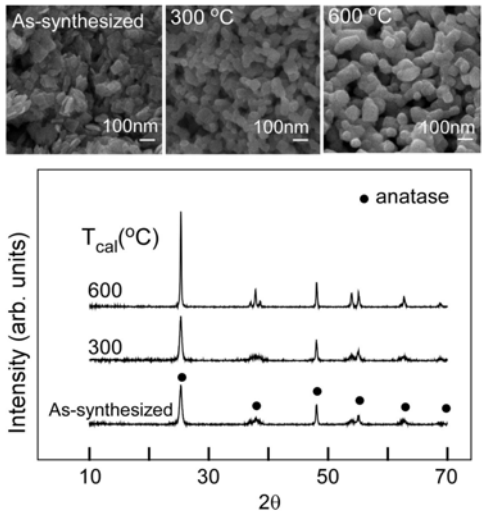

Figure 1. SEM images (upper) and XRD spectra (lower) of as-synthesized TiO_2 nanocrystals and those after calcination at 300 and 600°C.

3. Photoactivity measurements

Photo-oxidation rate of methylene blue (MB) were measured in an aqueous solution of MB (0.005～0.025 mM) with TiO_2 nanocrystals (0～0.03 g/L) suspended in it at RT. During the reaction, the pH was kept in the range of 5～6 and the absorbance at 665 nm was collected over time under the UV (15 W, 365 nm) irradiation. The variation of the absorbance (C) with respect to the initial absorbance (C_0) was used to obtain initial first-order rate constants (k) in units of min^{-1}, from a plot of ln (C_0/C) vs. reaction time (min). For a systematic evaluation of the photocatalytic reaction characteristics, either the MB concentration or the amount of TiO_2 was varied and the rate constants were monitored.

III. Results and Discussion

For a quantitative evaluation of photocatalytic properties of anatase TiO_2 nanocrystals of well-defined shapes, we have synthesized regular shaped TiO_2 nanocrystals by employing well-practiced synthetic approaches as shown in Fig. 1. The TiO_2 nanocrystals are in anatase phase as is clear from the sharp (101) and (200) peaks at 25 and 48°, respectively (see XRD spectrum in Fig. 1). After calcination at higher temperatures, the shape of the TiO_2 nanocrystals changes into thicker and larger nanocrystals (SEM images in Fig. 1) due to agglomerate of small

nanocrystals into bigger particles under the calcination condition [39]. XRD spectra also confirm such changes from the growth of sharper anatase peaks (XRD spectra in Fig. 1). As a result, the surface area of the TiO_2 nanocrystals gradually decreases from 68 m^2/g (for the as-synthesized TiO_2) to 56 m^2/g (after calcination at 600°C) as determined from the N_2 adsorption characteristics at liquid nitrogen temperature (BET measurements).

Since photocatalytic activity is strongly influenced by the presence of defects in oxide nanocrystals, we show EPR spectra of our TiO_2 nanocrystals in Fig. 2. The EPR spectrum of as-synthesized TiO_2 shows no signal, indicating no paramagnetic defect center exists in the oxide crystals. After calcination at 300°C, strong EPR signals appear at 1.96~2.01, which are attributed to the presence of O^- [40-42] and Ti^{3+} species [43-46]. The EPR spectra are taken at ambient condition and surfaces of TiO_2 may interact with O_2 as well as H_2O in the air to produce surface-bound species which can be paramagnetic such as O^- as can be detected from EPR in Fig. 2. In addition, the presence of Ti^{3+}-related EPR signals in Fig. 3 for those TiO_2 calcined at 300 and 600°C reflects that the growth of the TiO_2 nanocrystals into bigger particles during the calcination (Fig. 1) involves the generation of reduced Ti^{3+} species [47,48], diffusion into the bulk and reoxidation under the oxidizing environment. As the calcination temperature increases up to 600°C, the defect densities in the bulk as well as on the surface may be reduced as can be confirmed from the smaller EPR signals in Fig. 2. This variation in defect density of TiO_2 nanocrystals has a critical role in determining the overall photocatalytic activity of the oxide nanocrystals [49].

Photocatalytic activity of TiO_2 nanocrystals can be evaluated from photooxidation rate of organic dye such as MB in aqueous solution. It is known to involve ·OH radical species which are generated by photogenerated holes in TiO_2 and the kinetic rates are often assumed to follow first-order reaction kinetics [5-7]; that is, the reaction rates increase in proportion to the first power of the concentration of reactant (in this case, [MB]). However, the actual

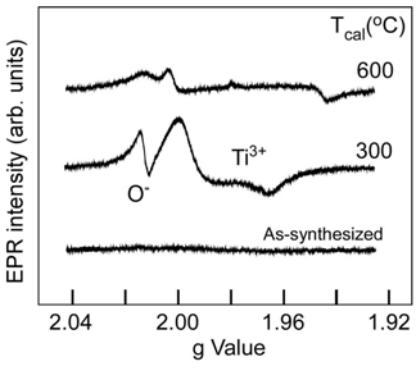

Figure 2. EPR spectra of as-synthesized TiO_2 nanocrystals and those after calcination at 300 and 600°C, respectively.

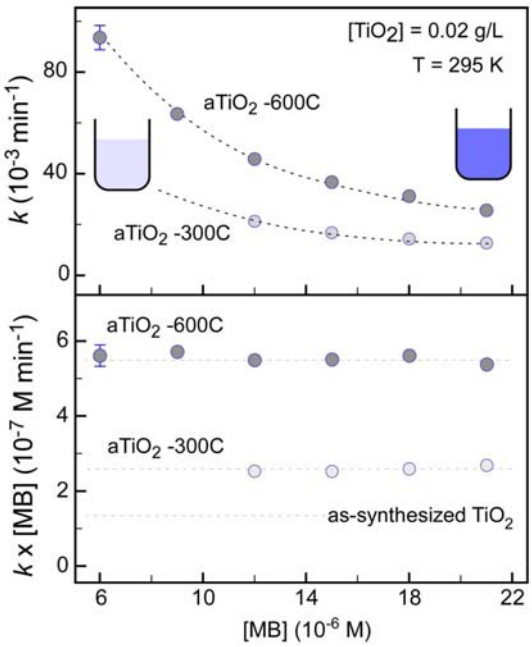

Figure 3. Photo-degradation rate constants (k, min^{-1}) plotted against MB concentration ([MB], 0.006~0.021 mM) for anatase TiO_2 nanocrystals after calcination at 300 and 600°C ($aTiO_2$-300C and $aTiO_2$-600C, respectively) (upper). Also, shown in the lower panel is the actual reaction rate (k×[MB]) plotted against [MB].

reaction kinetics may vary possibly due to the presence of other limiting factors. For example, as shown in Fig. 3, the rate constant determined from the photodegradation of MB under our given condition is observed to increase as the MB concentration decreases. By assuming first order kinetics, the actual reaction rate may be obtained by multiplying the MB concentration and k (as shown in the lower panel of Fig. 3). Interestingly, the result shows a constant reaction rate irrespective of the MB concentration. At first glance, it may look incorrect since the rate is thought to be first-order; that is, the rate is expected to increase in proportion to the MB concentration. However, the amount of TiO_2 in the aqueous solution is fixed to 0.02 g/L in this case. Here, the MB concentration is in an excess limit and the limiting factors in this case are the concentration of active sites on TiO_2 particles and the efficiency of generating catalytically active charge carriers as a result of UV absorption.

One more interesting observation in Fig. 3 is that higher reaction rates are obtained in an order of $aTiO_2$-600C > $aTiO_2$-300C > as-synthesized TiO_2. This observation, again, is understood from changes of those TiO_2 nanocrystals annealed to higher temperatures in shape and size [50-53], surface area [54], defect distribution and density [55-59], morphology and crystallinity. That is, *the measured photocatalytic reaction rate constant is not determined by the MB concentration*, *but represents the absolute efficiency (and the number) of those active sites on the TiO_2 surfaces* where photogenerated holes are used to induce oxidation of organic dyes.

The effect of increasing the amount of TiO_2 nanocrystals used is shown in Fig. 4. In this case, the rate constant is monitored as the TiO_2 concentration (g/L) is raised. It is shown to increase quite in proportion to the concentration up to about 0.004 g/L, but at higher TiO_2 concentrations, the effect of adding more TiO_2 gradually diminishes and the slope

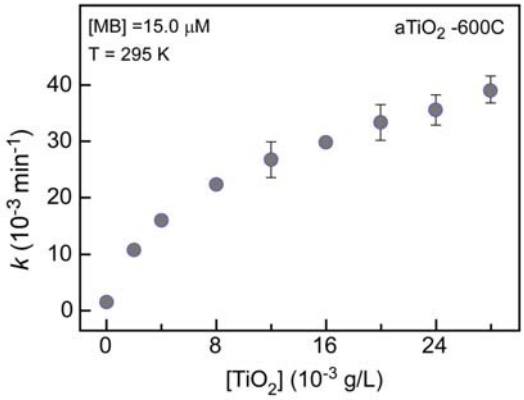

Figure 4. Photodegradation rates of MB over TiO_2 nanocrystals after calcination at 600°C (TiO_2-600C) plotted against the amount of TiO_2 ([TiO_2], 0 ~ 0.028 g/L) used. Here, [MB] was fixed to 15.0 μM.

becomes lower. At low TiO_2 concentration limit, the aqueous solution under UV illumination is quite transparent and the whole solution can be assumed to be exposed to the UV light. Adding white TiO_2 powders makes the solution murky and the depth under the UV exposure becomes shorter due to light scattering by TiO_2 particles. Shorter penetration depth of UV light may be compensated in part by the increased particle density in the solution to some extent. Here, the net effect is observed to be a gradual decrease in the contribution of added TiO_2 to the overall reaction rate.

IV. Conclusions

We have evaluated photocatalytic activity of anatase TiO_2 nanocrystals under UV irradiation by measuring photodegradation rate of MB in aqueous solution. The effect of concentration of catalysts (or reactants) is often complicated by the complex interplay among various contributions such as light scattering, diffusion of reactant and mysterious roles of different type of defects in photoexcited charge separation and reactions at active sites of TiO_2 surfaces. Here, our

results show that the experimental condition given for the evaluation of photocatalytic activity of TiO_2 in this case ensures that the overall photocatalytic reaction rate is limited by the concentration of TiO_2 nanoparticles which is closely related to the number of active sites for photooxidation reactions induced by photoexcited charge carriers.

Acknowledgements

This research was supported by Basic Science Research Program through the National Research Foundation of Korea (NRF) funded by the Ministry of Education, Science and Technology (NRF-2012R1A1A2 007641).

References

[1] M. Pelaez, et al., Appl. Catal. B **125**, 331 (2012).
[2] K. Nakata, A. Fujishima, Journal of Photochemistry and Photobiology C: Photochemistry Reviews **13**, 169 (2012).
[3] H. Park, Y. Park, W. Kim, W. Choi, Journal of Photochemistry and Photobiology C: Photochemistry Reviews **15**, 1 (2013).
[4] J. Su, X. Zou, J.-S. Chen, RSC Adv. **4**, 13979 (2014).
[5] A. Houas, H. Lachheb, M. Ksibi, E. Elaloui, C. Guillard, J.-M. Herrmann, Appl. Catal. B **31**, 145 (2001).
[6] H. Lachheb, E. Puzenat, A. Houas, M. Ksibi, E. Elaloui, C. Guillard, J.-M. Herrmann, Appl. Catal. B **39**, 75 (2002).
[7] C.-H. Wu, J.-M. Chern, Ind. Eng. Chem. Res. **45**, 6450 (2006).
[8] G.M. Madhu, M.A. Lourdu Antony Raj, K. Vasantha Kumar Pai, Journal of Environmental Biology **30**, 259 (2009).
[9] S. Chin, E. Park, M. Kim, J. Jurng, Powder Technology **201**, 171 (2010).
[10] M. Ni, M.K.H. Leung, D.Y.C. Leung, K. Sumathy, Renewable Sustainable Energy Rev. **11**, 401 (2007).
[11] A. Kudo, International Journal of Hydrogen Energy **32**, 2673 (2007).
[12] A. Fujishima, X. Zhang, D.A. Tryk, Surf. Sci. Rep. **63**, 515 (2008).
[13] A. Kudo, Y. Miseki, Chem. Soc. Rev. **38**, 253 (2009).
[14] K. Maeda, K. Domen, The Journal of Physical Chemistry Letters **1**, 2655 (2010).
[15] S. Ikeda, N. Sugiyama, S.-y. Murakami, H. Kominami, Y. Kera, H. Noguchi, K. Uosaki, T. Torimoto, B. Ohtani, Phys. Chem. Chem. Phys. **5**, 778 (2003).
[16] D.C. Hurum, K.A. Gray, T. Rajh, M.C. Thurnauer, J. Phys. Chem. B **109**, 977 (2004).
[17] M. D'Arienzo, J. Carbajo, A. Bahamonde, M. Crippa, S. Polizzi, R. Scotti, L. Wahba, F. Morazzoni, J. Am. Chem. Soc. **133**, 17652 (2011).
[18] X. Yu, B. Kim, Y.K. Kim, ACS Catal. **3**, 2479 (2013).
[19] X. Yu, B. Jeon, Y.K. Kim, ACS Catal. **5**, 3316 (2015).
[20] X. Zhao, W. Jin, J. Cai, J. Ye, Z. Li, Y. Ma, J. Xie, L. Qi, Adv. Funct. Mater. **21**, 3554 (2011).
[21] K. Hayashi, M. Nakamura, Y. Makita, R. Fujiwara, T. Kori, K. Ishimura, Mater. Lett. **65**, 3037 (2011).
[22] S. Auvinen, M. Alatalo, H. Haario, J.-P. Jalava, R.-J. Lamminmäki, J. Phys. Chem. C **115**, 8484 (2011).
[23] L. Wang, L. Zang, J. Zhao, C. Wang, Chem. Commun. **48**, 11736 (2012).
[24] X. Liu, H. Zhang, X. Yao, T. An, P. Liu, Y. Wang, F. Peng, A. Carroll, H. Zhao, Nano Res. **5**, 762 (2012).
[25] D. Wu, Z. Gao, F. Xu, J. Chang, S. Gao, K. Jiang, CrystEngComm **15**, 516 (2013).

[26] C. Deiana, M. Minella, G. Tabacchi, V. Maurino, E. Fois, G. Martra, Phys. Chem. Chem. Phys. **15**, 307 (2013).

[27] Q. Shi, Y. Li, E. Zhan, N. Ta, W. Shen, CrystEngComm **16**, 3431 (2014).

[28] J. Chen, B. Li, J. Zheng, S. Jia, J. Zhao, H. Jing, Z. Zhu, J. Phys. Chem. C **115**, 7104 (2011).

[29] Z. Sun, J.H. Kim, Y. Zhao, F. Bijarbooneh, V. Malgras, Y. Lee, Y.-M. Kang, S.X. Dou, J. Am. Chem. Soc. **133**, 19314 (2011).

[30] A.G. Kontos, M. Pelaez, V. Likodimos, N. Vaenas, D.D. Dionysiou, P. Falaras, Photochemical & Photobiological Sciences **10**, 350 (2011).

[31] C. Han, M. Pelaez, V. Likodimos, A.G. Kontos, P. Falaras, K. O'Shea, D.D. Dionysiou, Appl. Catal. B **107**, 77 (2011).

[32] I. Paramasivam, H. Jha, N. Liu, P. Schmuki, Small **8**, 3073 (2012).

[33] J. Bouclé, J. Ackermann, Polymer International **61**, 355 (2012).

[34] E.C. Landis, K.C. Phillips, E. Mazur, C.M. Friend, J. Appl. Phys. **112**, 063108 (2012).

[35] Y. Qu, X. Duan, Chem. Soc. Rev. **42**, 2568 (2013).

[36] J. Yu, J. Fan, K. Lv, Nanoscale **2**, 2144 (2010).

[37] Q. Xiang, K. Lv, J. Yu, Appl. Catal. B **96**, 557 (2010).

[38] Z. Wang, K. Lv, G. Wang, K. Deng, D. Tang, Appl. Catal. B **100**, 378 (2010).

[39] J. Zhang, M. Li, Z. Feng, J. Chen, C. Li, J. Phys. Chem. B **110**, 927 (2006).

[40] J. Strunk, W.C. Vining, A.T. Bell, J. Phys. Chem. C **114**, 16937 (2010).

[41] W. Wang, C. Lu, Y. Ni, M. Su, Z. Xu, Appl. Catal. B **127**, 28 (2012).

[42] T. Thompson, J. Yates, Jr., Top. Catal. **35**, 197 (2005).

[43] C.P. Kumar, N.O. Gopal, T.C. Wang, M.-S. Wong, S.C. Ke, J. Phys. Chem. B **110**, 5223 (2006).

[44] X. Liu, S. Gao, H. Xu, Z. Lou, W. Wang, B. Huang, Y. Dai, Nanoscale **5**, 1870 (2013).

[45] H. Liu, H.T. Ma, X.Z. Li, W.Z. Li, M. Wu, X.H. Bao, Chemosphere **50**, 39 (2003).

[46] J. Cunningham, A.L. Penny, J. Phys. Chem. **78**, 870 (1974).

[47] G. Lu, A. Linsebigler, J.T. Yates, J. Phys. Chem. **98**, 11733 (1994).

[48] M. Bowker, R.A. Bennett, J. Phys. Condens. Matt. **21**, 474224 (2009).

[49] M. Kong, Y. Li, X. Chen, T. Tian, P. Fang, F. Zheng, X. Zhao, J. Am. Chem. Soc. **133**, 16414 (2011).

[50] N. Murakami, Y. Kurihara, T. Tsubota, T. Ohno, J. Phys. Chem. C **113**, 3062 (2009).

[51] I. Lee, F. Delbecq, R. Morales, M.A. Albiter, F. Zaera, Nat Mater **8**, 132 (2009).

[52] C.-K. Tsung, J.N. Kuhn, W. Huang, C. Aliaga, L.-I. Hung, G.A. Somorjai, P. Yang, J. Am. Chem. Soc. **131**, 5816 (2009).

[53] C.-T. Dinh, T.-D. Nguyen, F. Kleitz, T.-O. Do, ACS Nano **3**, 3737 (2009).

[54] T. Froschl, et al., Chem. Soc. Rev. **41**, 5313 (2012).

[55] E. Lira, S. Wendt, P. Huo, J.Ø. Hansen, R. Streber, S. Porsgaard, Y. Wei, R. Bechstein, E. Lægsgaard, F. Besenbacher, J. Am. Chem. Soc. **133**, 6529 (2011).

[56] J. Yan, G. Wu, N. Guan, L. Li, Z. Li, X. Cao, Phys. Chem. Chem. Phys. **15**, 10978 (2013).

[57] Q. Zhu, Y. Peng, L. Lin, C.-M. Fan, G.-Q. Gao, R.-X. Wang, A.-W. Xu, J. Mater. Chem. A **2**, 4429 (2014).

[58] Y. Yan, M. Han, A. Konkin, T. Koppe, D. Wang, T. Andreu, G. Chen, U. Vetter, J.R. Morante, P. Schaaf, J. Mater. Chem. A **2**, 12708 (2014).

[59] L. Li, J. Yan, T. Wang, Z.-J. Zhao, J. Zhang, J. Gong, N. Guan, Nat Commun **6**, 5881 (2015).